An IIR Youla-Kucera parametrized adaptive feedforward compensator for active vibration control with mechanical coupling

Ioan Doré Landau, Tudor-Bogdan Airimiţoaie and Marouane Alma

Abstract— Adaptive feedforward broadband vibration (or noise) compensation is currently used when a measurement correlated with the disturbance is available. However, in most of the systems there is a "positive" feedback coupling between the compensator system and the disturbance correlated measurement. This may lead to the instability of the system. The paper proposes a new Youla-Kucera (YK) parametrization of the compensator. The central compensator assures the stability of the system and its performances are enhanced in real time by the adaptation of the parameters of an IIR Youla-Kucera filter. An analysis of the resulting system is provided. The results of this paper on one hand generalize previous results obtained for FIR Youla-Kucera adaptive filters and on the other hand lead to a significant reduction of the number of parameter to be adapted for the same level of performance. The algorithm has been applied to an Active Vibration Control (AVC) system and real time results are presented.

Index Terms— active vibration control, adaptive feedforward compensation, adaptive control, Youla-Kucera parametrization, parameter estimation.

I. INTRODUCTION

Adaptive feedforward broadband vibration (or noise) compensation is currently used in ANC (Active Noise Control) and AVC when an image of the disturbance (i.e. a correlated measurement) is available ([3], [4], [7], [16]). However, in many systems there is a "positive" feedback coupling between the compensator system and the measurement of the image of the disturbance (vibration or noise) ([6], [7], [16]). The positive feedback may destabilize the system because the system is no more a pure feedforward compensator.

Different solutions have been proposed to overcome this problem (see for example [8]). In [7], [10] algorithms for adapting the IIR feedforward filter in real time taking into account the presence of the positive feedback have been proposed, analyzed and evaluated. In [15] the FULMS algorithm is analyzed in the context of this internal positive feedback. An experimental evaluation of these various approaches can be found in [10].

In [16], the idea of using an YK parametrization of the feedforward compensator is illustrated in the context of ANC. Based on the identification of the system, a stabilizing YK controller using an orthonormal basis filter is designed. The YK parameters weighting the orthonormal basis filters are then updated by using a two time scale indirect procedure: (1) estimation of the Q-filter's parameters over a certain

Ioan Doré Landau, Tudor-Bogdan Airimiţoaie and Marouane Alma are with the Control system department of GIPSA-Lab, St. Martin d'Héres, 38402 FRANCE Ioan-Dore.Landau@gipsa-lab.grenoble-inp.fr

horizon, (2) updating of the controller. No stability proof for the tuning procedure is provided.

In [9] an algorithm for adapting the Q parameters of an FIR Youla-Kucera (also called QFIR) parameterized feedforward compensator has been proposed, analyzed and tested experimentally on an AVC system. While the central stabilizing compensator has a IIR structure, the YK filter has an FIR structure.

The main contributions of this paper with respect to [9], [16] are:

- the development of a new real time recursive adaptation algorithm for the Q-parameters of a QIIR filter and the analysis of the stability of the resulting system;
- experimental and simulation comparison with adaptive feedforward compensators using a QFIR filter;
- reduction of the number of parameters to be adapted for the same level of performance.

While the paper is developed in the context of AVC, the results are certainly applicable to ANC systems.

The paper is organized as follows. In Section II the AVC system which will be used as a test bench will be presented. The system representation and feedforward filter structure are given in section III. The algorithm for adaptive feedforward compensation will be developed in section IV and analyzed in section V. Section VI will present simulated and experimental results obtained on the AVC system.

II. AN AVC SYSTEM USING AN INERTIAL ACTUATOR
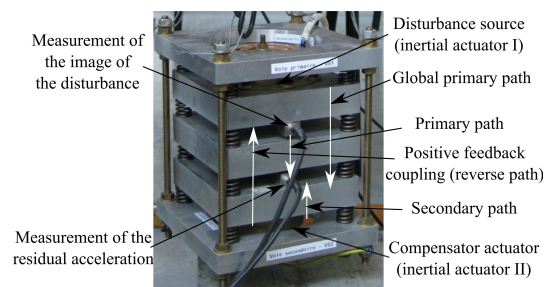
Fig. 1. An AVC system using a feedforward compensation - photo

Figures 1 and 2 represent an AVC system using a measurement of the image of the disturbance and an inertial actuator for reducing the residual acceleration. It consists of five metal plates connected by springs, out of which the first and last being fixed form the support. The second and fourth plates are equipped with an inertial actuator: the first will excite the structure (disturbances) and the second will create vibrational
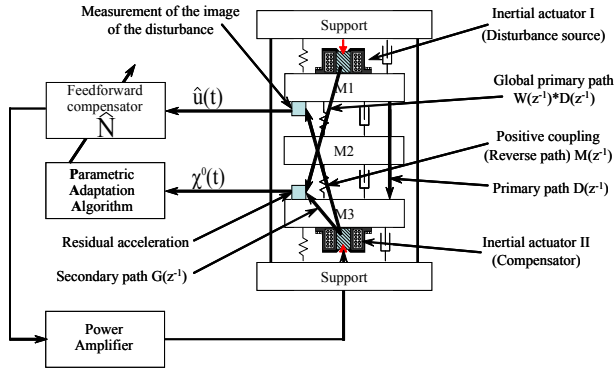
Fig. 2. An AVC system using a feedforward compensation - scheme

forces which can counteract the effect of these vibrational disturbances. The image of the disturbance and the residual acceleration are measured by accelerometers.

The path between the disturbance and the residual acceleration is called the *global primary path*, the path between the measure of the image of the disturbance and the residual acceleration (in open loop) is called the *primary path* and the path between the inertial actuator and the residual acceleration is called the *secondary path*. $d(t)$ is the image of the disturbance measured effectively when the compensator system is not used. When the compensator system is active, the actuator acts upon the residual acceleration, but also upon the measurement of the image of the disturbance. The measured quantity will be the sum of the disturbance $d(t)$ and of the effect of the actuator. The problem of "positive" feedback coupling is clearly illustrated in figures 1 and 2. ([7], [16]).

(a)

(b)
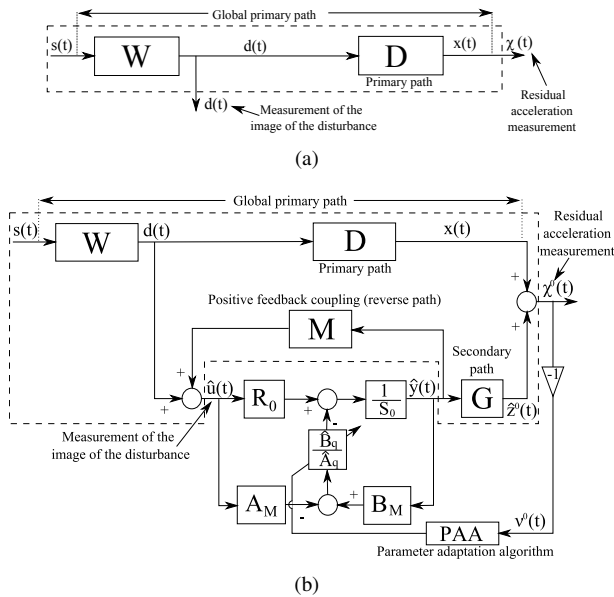
Fig. 3. Feedforward AVC: in open loop (a) and with adaptive feedforward compensator (b)

The input to the inertial actuators being a position, the global primary path, the secondary path and the positive

feedback path have a double differentiator behavior. The corresponding block diagrams in open loop operation and with the compensator system are shown in Figures 3(a) and 3(b). $\hat{u}(t)$ denotes the effective output provided by the measurement device and which will serve as input to the adaptive feedforward filter $\hat{N}$. The output of this filter denoted by $\hat{y}(t)$ is applied to the actuator through an amplifier. The transfer function G (the secondary path) characterizes the dynamics from the output of the filter $\hat{N}$ to the residual acceleration measurement (amplifier + actuator + dynamics of the mechanical system). The transfer function D between $d(t)$ and the measurement of the residual acceleration (in open loop operation) characterizes the primary path.

The "positive" coupling between the output of the filter and the measurement $\hat{u}(t)$ through the compensator actuator is denoted by M.

At this stage it is important to mention that in the absence of the feedforward filter very reliable models for the secondary path, the "positive" feedback path and the primary path can be identified by applying appropriate excitation on the actuator.

III. BASIC EQUATIONS AND NOTATIONS

The different blocks of the AVC system will be described in this section. The primary (D), secondary (G) and reverse (positive coupling) (M) paths represented in (3(b)) are characterized by the asymptotically stable transfer operators[1]:

$$D(q^{-1}) = \frac{B_D(q^{-1})}{A_D(q^{-1})} = \frac{b_1^D q^{-1} + ... + b_{n_{B_D}}^D q^{-n_{B_D}}}{1 + a_1^D q^{-1} + ... + a_{n_{A_D}}^D q^{-n_{A_D}}}, \quad (1)$$

$$G(q^{-1}) = \frac{B_G(q^{-1})}{A_G(q^{-1})} = \frac{b_1^G q^{-1} + ... + b_{n_{B_G}}^G q^{-n_{B_G}}}{1 + a_1^G q^{-1} + ... + a_{n_{A_G}}^G q^{-n_{A_G}}}, \quad (2)$$

$$M(q^{-1}) = \frac{B_M(q^{-1})}{A_M(q^{-1})} = \frac{b_1^M q^{-1} + ... + b_{n_{B_M}}^M q^{-n_{B_M}}}{1 + a_1^M q^{-1} + ... + a_{n_{A_M}}^M q^{-n_{A_M}}}. \quad (3)$$

The optimal feedforward filter (unknown) is defined by

$$N(q^{-1}) = \frac{R(q^{-1})}{S(q^{-1})} = \frac{r_0 + r_1 q^{-1} + ... + r_{n_R} q^{-n_R}}{1 + s_1 q^{-1} + ... + s_{n_S} q^{-n_S}} \quad (4)$$

For the purpose of this paper, an Youla-Kucera parametrization of the optimal filter is considered ([2]). In this case, the filter polynomials $R(q^{-1})$ and $S(q^{-1})$ become:

$$R(q^{-1}) = A_Q(q^{-1}) R_0(q^{-1}) - B_Q(q^{-1}) A_M(q^{-1}), \quad (5)$$
$$S(q^{-1}) = A_Q(q^{-1}) S_0(q^{-1}) - B_Q(q^{-1}) B_M(q^{-1}) \quad (6)$$

where $S_0(q^{-1})$ and $R_0(q^{-1})$ denote respectively the denominator and numerator of the central (stabilizing) controller and $A_Q(q^{-1})$ and $B_Q(q^{-1})$ are the denominator and the numerator of the optimal Q filter

$$Q(q^{-1}) = \frac{B_Q(q^{-1})}{A_Q(q^{-1})} = \frac{b_0^Q + b_1^Q q^{-1} + ... + b_{n_{B_Q}}^Q q^{-n_{B_Q}}}{1 + a_1^Q q^{-1} + ... + a_{n_{A_Q}}^Q q^{-n_{A_Q}}}. \quad (7)$$

The estimated filter is denoted by $\hat{N}(q^{-1})$. The estimated Q filter is denoted by $\hat{Q}(q^{-1})$ or $\hat{Q}(\hat{\theta}, q^{-1})$ when it is a linear

---

[1]The parenthesis (q^{-1}) will be omitted in some of the following equations to make them more compact.

filter with constant coefficients or $\hat{Q}(t,q^{-1})$ during estimation (adaptation). Similarly the estimated polynomials R and S will be denoted $\hat{R}(t,q^{-1})$ and $\hat{S}(t,q^{-1})$.

The input-output relationships for the estimated feedforward filter for the case of time varying parameter estimates are given by the "a priori" output

$$\hat{y}^0(t+1) = -\hat{S}^*(t,q^{-1})\hat{y}(t) + \hat{R}(t,q^{-1})\hat{u}(t+1) \qquad (8)$$

where $\hat{S}^*(t,q^{-1})$ and $\hat{R}(t,q^{-1})$ satisfy equations (5) and (6) in which Q is replaced by $\hat{Q}(t,q^{-1})$ and $\hat{y}(t)$, $\hat{y}(t-1)$, ... are the "a posteriori" outputs of the feedforward filter generated by

$$\hat{y}(t+1) = -\hat{S}^*(t+1,q^{-1})\hat{y}(t) + \hat{R}(t+1,q^{-1})\hat{u}(t+1). \qquad (9)$$

The measured input to the feedforward filter satisfies the following equation (in adaptive operation)

$$\hat{u}(t) = d(t) + \frac{B_M(q^{-1})}{A_M(q^{-1})}\hat{y}(t) \qquad (10)$$

Note that in the case of constant parameters one has $\hat{y}(t) = \hat{y}$.

The "a posteriori" unmeasurable value of the output of the secondary path is denoted by $\hat{z}(t)$ while its input is $\hat{y}(t)$. The "a priori" output of the secondary path will be denoted $\hat{z}^0(t)$. One has:

$$\hat{z}(t) = G(q^{-1})\hat{y}(t); \quad \hat{z}^0(t) = G(q^{-1})\hat{y}^0(t) \qquad (11)$$

The measured residual acceleration (or force) satisfies the following equation

$$\chi^0(t) = x(t) + \hat{z}^0(t) \qquad (12)$$

The "a priori" adaptation error is given by:

$$v^0(t) = -\chi^0(t) \qquad (13)$$

The "a posteriori" unmeasurable (but computable) adaptation error is given by:

$$v(t) = -x(t) - \hat{z}(t) \qquad (14)$$

For compensators with constant parameters $v^0(t) = v(t)$.

IV. Algorithm development

The algorithm for adaptive feedforward compensation will be developed under the following hypotheses:

1) The signal $d(t)$ is bounded (which is equivalently to say that $s(t)$ is bounded and $W(q^{-1})$ in figure 3 is asymptotically stable).
2) It exists a central feedforward compensator $N_0(R_0,S_0)$ which stabilizes the inner positive feedback loop formed by N_0 and M and the characteristic polynomial of the closed loop:

$$P_0(z^{-1}) = A_M(z^{-1})S_0(z^{-1}) - B_M(z^{-1})R_0(z^{-1}) \qquad (15)$$

is a Hurwitz polynomial.
3) (Perfect matching condition) It exists a value of the Q parameters such that

$$\frac{G \cdot A_M(R_0 A_Q - A_M B_Q)}{A_Q(A_M S_0 - B_M R_0)} = -D. \qquad (16)$$

4) The effect of the measurement noise upon the measurement of the residual acceleration is neglected (deterministic context).

Once the algorithm will be developed under these hypotheses, hypotheses 3 and 4 will be removed and the algorithm will be analyzed in this modified context.

A first step in the development of the algorithms is to establish for a fixed estimated compensator a relation between the error on the Q-parameters (with respect to the optimal values) and the adaptation error v. This is summarized in the following lemma:

Lemma 4.1: *Under the hypothesis 1 through 4 for the system described in figure 3 using a Q-parameterized feedforward compensator with constant parameters one has:*

$$v(t+1) = \frac{A_M(q^{-1})G(q^{-1})}{A_Q(q^{-1})P_0(q^{-1})}[\theta - \hat{\theta}]^T\phi(t), \qquad (17)$$

where

$$\theta^T = [b_0^Q,\ldots,b_{n_{B_Q}}^Q, a_1^Q,\ldots,a_{n_{A_Q}}^Q] = [\theta_{B_Q}^T, \theta_{A_Q}^T] \qquad (18)$$

is the vector of parameters of the optimal Q filter assuring perfect matching,

$$\hat{\theta}^T = [\hat{b}_0^Q,\ldots,\hat{b}_{n_{B_Q}}^Q, \hat{a}_1^Q,\ldots,\hat{a}_{n_{A_Q}}^Q] = [\hat{\theta}_{B_Q}^T, \hat{\theta}_{A_Q}^T] \qquad (19)$$

is the vector of parameters for the estimated $\hat{Q}$ filter

$$\hat{Q}(q^{-1}) = \frac{\hat{B}_Q(q^{-1})}{\hat{A}_Q(q^{-1})} = \frac{\hat{b}_0^Q + \hat{b}_1^Q q^{-1} + \ldots + \hat{b}_{n_{B_Q}}^Q q^{-n_{B_Q}}}{1 + \hat{a}_1^Q q^{-1} + \ldots + \hat{a}_{n_{A_Q}}^Q q^{-n_{A_Q}}} \qquad (20)$$

and $\alpha(t+1)$, $\beta(t)$ and ϕ are given respectively by:

$$\alpha(t+1) = B_M^*\hat{y}(t) - A_M\hat{u}(t+1) \qquad (21a)$$
$$\beta(t) = R_0\hat{u}(t) - S_0\hat{y}(t) \qquad (21b)$$
$$\phi^T(t) = [\alpha(t+1), \alpha(t),\ldots,\alpha(t-n_{B_Q}+1),$$
$$\beta(t), \beta(t-1),\ldots,\beta(t-n_{A_Q})]. \qquad (21c)$$

Proof: See appendix I.

Remark: This result can be particularized for the case of a FIR Youla Kucera filter by taking $A_Q = 1$ and $\hat{A}_Q = 1$.

Filtering the vector ϕ by an asymptotically stable filter $L(q^{-1})$, eq. (17) becomes:

$$v(t+1) = \frac{A_M(q^{-1})G(q^{-1})}{A_Q P_0(q^{-1})L(q^{-1})}[\theta - \hat{\theta}]^T\phi_f(t) \qquad (22)$$

with

$$\phi_f(t) = L(q^{-1})\phi(t) = [\alpha_f(t+1), \alpha_f(t),\ldots,\alpha(_f t-n_{B_Q}+1),$$
$$\beta_f(t), \beta_f(t-1),\ldots,\beta_f(t-n_{A_Q})] \qquad (23)$$

where

$$\alpha_f(t+1) = L(q^{-1})\alpha(t+1),$$
$$\beta_f(t) = L(q^{-1})\beta(t). \qquad (24)$$

Eq. (22) will be used to develop the adaptation algorithms.

For the case in which the parameters of $\hat{Q}$ evolve over time, and neglecting the non-commutativity of the time varying operators, equation (22) transforms into the equation of the *a posteriori* adaption error[2]

$$v(t+1) = \frac{A_M(q^{-1})G(q^{-1})}{A_Q(q^{-1})P_0(q^{-1})L(q^{-1})}[\theta - \hat{\theta}(t+1)]^T\phi_f(t). \qquad (25)$$

[2]However exact algorithms can be developed taking into account the non-commutativity of the time varying operators - see [13].

Equation (25) has the standard form for an "a posteriori adaption error equation ([13]), which immediately suggests to use the following parameter adaptation algorithm:

$$\hat{\theta}(t+1) = \hat{\theta}(t) + F(t)\Phi(t)\nu(t+1) \tag{26a}$$

$$\nu(t+1) = \frac{\nu^0(t+1)}{1 + \Phi^T(t)F(t)\Phi(t)} \tag{26b}$$

$$F(t+1) = \frac{1}{\lambda_1(t)}\left[F(t) - \frac{F(t)\Phi(t)\Phi^T(t)F(t)}{\frac{\lambda_1(t)}{\lambda_2(t)} + \Phi^T(t)F(t)\Phi(t)}\right] \tag{26c}$$

$$1 \geq \lambda_1(t) > 0; 0 \leq \lambda_2(t) < 2; F(0) > 0 \tag{26d}$$

$$\Phi(t) = \phi_f(t) \tag{26e}$$

where $\lambda_1(t)$ and $\lambda_2(t)$ allow to obtain various profiles for the matrix adaptation gain $F(t)$ (see [13]). By taking $\lambda_2(t) \equiv 0$ one gets a constant adaptation gain matrix (and choosing $F = \gamma I$, $\gamma > 0$ one gets a scalar adaptation gain). The measured *a priori* adaptation error is given by (13).

Three choices for the filter L will be considered, leading to three different algorithms:

Algorithm *I*: $L = G$.
Algorithm *II*: $L = \hat{G}$.
Algorithm *III*: $L = \frac{\hat{A}_M}{\hat{P}}\hat{G}$,
where $\hat{P} = \hat{A}_Q(\hat{A}_M\hat{S}_0 - \hat{B}_M\hat{R}_0) = \hat{A}_Q\hat{P}_0$.

V. ANALYSIS OF THE ALGORITHMS

A. The deterministic case - perfect matching

Equation (25) for the a posteriori adaptation error has the form:

$$\nu(t+1) = H(q^{-1})[\theta - \hat{\theta}(t+1)]^T\Phi(t) \tag{27}$$

where

$$H(q^{-1}) = \frac{A_M(q^{-1})G(q^{-1})}{A_Q(q^{-1})P_0(q^{-1})L(q^{-1})}, \Phi = \phi_f \tag{28}$$

One has the following result:

Lemma 5.1: *Assuming that eq. (27) represents the evolution of the a posteriori adaption error and that the parameter adaption algorithm (26a) through (26e) is used one has*:

$$\lim_{t\to\infty}\nu(t+1) = 0 \tag{29}$$

$$\lim_{t\to\infty}\frac{[\nu^0(t+1)^2]}{1+\Phi(t)^TF(t)\Phi(t)} = 0 \tag{30}$$

$$||\Phi(t)|| \text{ is bounded} \tag{31}$$

$$\lim_{t\to\infty}\nu^0(t+1) = 0 \tag{32}$$

for any initial conditions $\hat{\theta}(0)$, $\nu(0)$ provided that:

$$H'(z^{-1}) = H(z^{-1}) - \frac{\lambda_2}{2}, \max_t[\lambda_2(t)] \leq \lambda_2 < 2 \tag{33}$$

is a strictly positive real transfer function.

Remark: This result can be particularized for the case of FIR Youla Kucera adaptive filters by taking $A_Q = 1$ and $\hat{A}_Q = 1$. The adaptation algorithm given by (26a) through (26e) is used with $\beta(t-i) = 0$, $i = 0,1,....$ and $\hat{a}_i^Q = 0$, $i = 1,2,....$.

Proof: To prove (29) and (30), one can straightforwardly use theorem 3.3.2 from [13] (pages 97-103).

However in order to show that $\nu^0(t+1)$ goes to zero one has to show first that the components of the regressor vector

are bounded. The result (30) suggests to use the Goodwin's "bounded growth" lemma ([5] and lemma 11.2.1 in [13] pg. 375). Provided that:

$$|\Phi^T(t)F(t)\Phi(t)|^{\frac{1}{2}} \leq C_1 + C_2.\max|\nu^0(k)| \tag{34}$$

$$0 < C_1 < \infty \quad 0 < C_2 < \infty \quad 0 \leq k \leq t+1, \quad F(t) > 0$$

$||\Phi(t)||$ will be bounded. So it will be shown that (34) holds.

This will be proved for algorithm I (for algorithms II and III, the proof is similar). From (14) one has:

$$-\hat{z}(t) = \nu(t) + x(t) \tag{35}$$

Since $x(t)$ is bounded (output of an asymptotically stable system with bounded input), one has:

$$|\hat{y}_f(t)| = |G\hat{y}(t)| = |\hat{z}(t)| \leq C_3 + C_4 \cdot \max_{0 \leq k \leq t+1}|\nu(k)|$$
$$\leq C_3' + C_4' \cdot \max_{0 \leq k \leq t+1}|\nu^0(k)| \tag{36}$$

since $|\nu(t)| \leq |\nu^0(t)|$ for all t. From (10) by multiplying both sides by $G(q^{-1})$ one gets in the adaptive case:

$$\hat{u}_f(t) = G(q^{-1})d(t) + \frac{B_M(q^{-1})}{A_M(q^{-1})}\hat{y}_f(t) \tag{37}$$

Since A_G and A_M are Hurwitz polynomials and that $d(t)$ is bounded, it results that:

$$|\hat{u}_f(t)| \leq C_5 + C_6 \cdot \max_{0 \leq k \leq t+1}|\nu^0(k)| \tag{38}$$

Using equations (21a), (21b), (24), (36) and (38) one can conclude that

$$|\alpha_f(t)| \leq C_7 + C_8 \cdot \max_{0 \leq k \leq t+1}|\nu^0(k)| \tag{39}$$

and

$$|\beta_f(t)| \leq C_9 + C_{10} \cdot \max_{0 \leq k \leq t+1}|\nu^0(k)| \tag{40}$$

Therefore (34) holds, which implies that $\Phi(t)$ is bounded and one can conclude that (32) also holds. End of the proof.

For Algorithm *I* one has:

$$H(q^{-1}) = \frac{A_M(q^{-1})}{A_Q(q^{-1})P_0(q^{-1})} \tag{41}$$

for Algorithm *II*, one has:

$$H(q^{-1}) = \frac{A_M(q^{-1})}{A_Q(q^{-1})P_0(q^{-1})} \cdot \frac{G(q^{-1})}{\hat{G}(q^{-1})} \tag{42}$$

and for Algorithm *III* one has:

$$H(q^{-1}) = \frac{A_M}{\hat{A}_M} \cdot \frac{\hat{A}_Q}{A_Q} \cdot \frac{\hat{P}_0}{P_0} \cdot \frac{G}{\hat{G}} \tag{43}$$

It is interesting to remark that for Algorithm *III*, the stability condition is that the transfer function:

$$\frac{A_M}{\hat{A}_M} \cdot \frac{\hat{A}_Q}{A_Q} \cdot \frac{\hat{P}_0}{P_0} \cdot \frac{G}{\hat{G}} - \frac{\lambda_2}{2} \tag{44}$$

should be strictly positive real. However this condition can be re-written for $\lambda_2 = 1$ as ([14]):

$$\left|\left(\frac{A_M}{\hat{A}_M} \cdot \frac{\hat{A}_Q}{A_Q} \cdot \frac{\hat{P}_0}{P_0} \cdot \frac{G}{\hat{G}}\right)^{-1} - 1\right| < 1 \tag{45}$$

for all ω. This roughly means that it always holds provided that the estimates of A_M, A_Q, P_0, and G are close to the true values (i.e. $H(e^{j\omega})$ in this case is close to a unit transfer function).

B. The stochastic case - perfect matching

Following the methodology given in [13] and [10], it can be shown that under the same "positive real" conditions as in the deterministic case the parameter estimations will be unbiased (provided that the measurement noise is independent of $d(t)$).

C. The case of non-perfect matching

If $\hat{N}(t, q^{-1})$ does not have the appropriate dimension there is no chance to satisfy the perfect matching condition. The results from [11], [12] can be used to analyze the boundedness of the residual error. It can be shown that all the signals are norm bounded under the passivity condition (33), where P is computed now with the reduced order estimated filter.

VI. EXPERIMENTAL RESULTS

The AVC system has been described in section II.

A. System identification
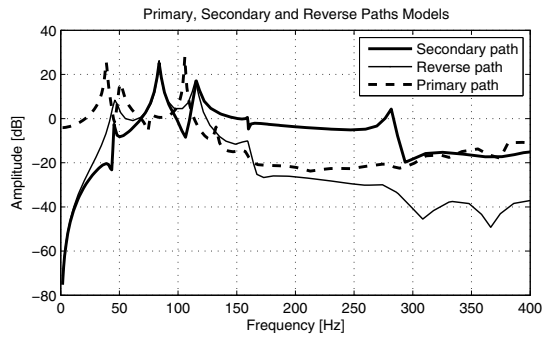
Fig. 4. Frequency characteristics of the primary, secondary and reverse paths

The structure of the linear discrete time models for the different paths have been given in section III. These models can be identified using the same methodology as in [12]. The excitation signal used to identify the different paths of the system was a PRBS (pseudo-random binary sequence). More details can be found in [10].

The estimated orders of the secondary and reverse paths are: $n_{B_G} = 17, n_{A_G} = 15, n_{B_M} = 16, n_{A_M} = 16$. The estimated orders of the model for the primary path are $n_{B_D} = 26, n_{A_D} = 26$. The frequency characteristics of the various paths are shown in figure 4. Note that the primary path features a strong resonance at 108 Hz, exactly where the secondary path has a pair of low damped complex zeros. Therefore one can not expect good attenuation around this frequency. A sampling frequency of $800\,Hz$ has been used.

B. The central controllers

Two central controllers have been considered. The first (PP) has been designed using a pole placement method. Its objective is to stabilize the internal positive feedback loop. The orders of the controller are: $n_{R_0} = 15$ and $n_{S_0} = 17$. The second (H_∞) is a reduced order[3] H_∞ controller with $n_{R_0} = 19$ and $n_{S_0} = 20$ from [1].

C. Comparative evaluation of QFIR and QIIR adaptive compensators

For comparison purposes the Algorithm *III* with decreasing adaptation gain applied for the case of a stationary disturbance with unknown characteristics has been considered. As disturbance, $s(t)$, a PRBS signal has been used. The implementation of the Algorithm *III* requires an estimation of $\hat{A}_Q$ which is in generally not available at the beginning. The algorithm is started with $\hat{A}_Q = 1$ and after an initialization horizon, one uses in the filter the current value of $\hat{A}_Q$ (for the presented experiments the initialization horizon was 150*s*).

No. of adap. parameters	8	16	32
QFIR/H_∞	13.69 dB	15.26 dB	15.90 dB
QFIR/PP	14.41 dB	15.81 dB	17.68 dB
QIIR/H_∞	17.51 dB	18.00 dB	19.46 dB
QIIR/PP	19.70 dB	20.63 dB	22.38 dB

TABLE I

DEPENDENCE OF THE GLOBAL ATTENUATION ON THE ORDER OF THE Q-POLYNOMIAL(SIMULATION)

The influence of the number of the adapted parameters on the global attenuation in simulation is illustrated in Table I. The major observation is that using QIIR the number of adapted parameters can be reduced drastically with respect to QFIR for the same level of attenuation.
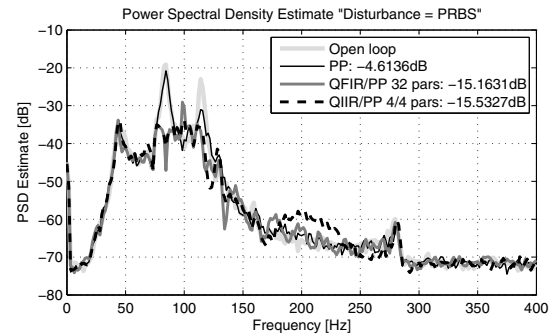
Fig. 5. Power spectral density estimates obtained using the PP controller (experimental)

The significantly better efficiency of the QIIR adaptive filter with respect to QFIR adaptive filters have been confirmed also by experimentations. Power spectral densities using the PP central controller are shown in fig. 5. One can observe that the QIIR algorithm with 8 (4/4) parameters gives a slightly better attenuation (15.53 *dB*) than the QFIR with 32 parameters (15.16 *dB*). Similar results are also obtained using the H_∞ central controller. The results can be viewed in fig. 6. The QIIR algorithm with 8 (4/4) parameters gives 16.53 *dB* while the QFIR algorithm gives 16.52 *dB*.

[3]The orders of the initial H_∞ controller were: $n_{R_{H_\infty}} = 70$ and $n_{S_{H_\infty}} = 70$.
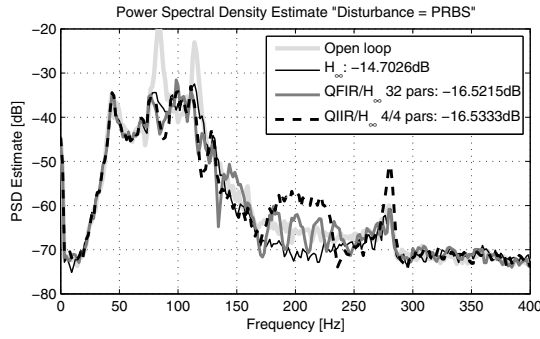
Fig. 6. Power spectral density estimates obtained using the H_∞ controller (experimental)

VII. CONCLUSIONS

The paper has presented an adaptive IIR Youla Kucera parametrized feedforward compensator built around a stabilizing filter for the internal "positive" feedback loop occurring in AVC and ANC systems. Experimental results on an Active Vibration Control system featuring an internal "positive" feedback have illustrated the potential of the approach. It has been shown that the use of the IIR Youla Kucera filters allows to reduce significantly the number of parameters to be adapted with respect to the FIR Youla Kucera [9] for the same level of performance.

APPENDIX I
PROOF OF LEMMA 4.1

We start by considering hypothesis 3, which suggests considering an equivalent closed loop system representation of the primary path. Considering a $Q(q^{-1})$ filter as in eq. (7), the polynomial $S(q^{-1})$ can be rewritten as

$$S(q^{-1}) = 1 + q^{-1}S^* = 1 + q^{-1}((A_Q S_0)^* - B_Q B_M^*). \quad (46)$$

Under hypothesis 3 (perfect matching condition) the output of the primary path can be expressed as

$$x(t) = -z(t) = -G(q^{-1})y(t) \quad (47)$$

and the input to the Youla-Kucera schema as

$$u(t+1) = d(t+1) + \frac{B_M}{A_M}y(t+1) \quad (48)$$

where $y(t)$ is a dummy variable given by

$$
\begin{aligned}
y(t+1) &= -S^*y(t) + Ru(t+1) \\
&= -((A_Q S_0)^* - B_Q B_M^*)y(t) + (A_Q R_0 - B_Q A_M)u(t+1) \\
&= -(A_Q S_0)^*y(t) + A_Q R_0 u(t+1) + B_Q(B_M^*y(t) - A_M u(t+1)).
\end{aligned}
\quad (49)
$$

Similarly, the output of the adaptive feedforward filter (for a fixed $\hat{Q}$) is given by

$$\hat{y}(t+1) = -(\hat{A}_Q S_0)^*\hat{y}(t) + \hat{A}_Q R_0 \hat{u}(t+1) + \hat{B}_Q(B_M^*\hat{y}(t) - A_M \hat{u}(t+1)). \quad (50)$$

The output of the secondary path is

$$\hat{z}(t) = G(q^{-1})\hat{y}(t). \quad (51)$$

Define the dummy error (for a fixed estimated set of parameters)

$$\varepsilon(t) = -y(t) + \hat{y}(t) \quad (52)$$

and the residual error

$$\nu(t) = -\chi(t) = -(-z(t) + \hat{z}(t)) = -G(q^{-1})\varepsilon(t)). \quad (53)$$

Equation (49) can be rewritten as

$$
\begin{aligned}
y(t+1) &= -(A_Q S_0)^*\hat{y}(t) + A_Q R_0 \hat{u}(t+1) + B_Q(B_M^*\hat{y}(t) - A_M \hat{u}(t+1)) \\
&\quad - (A_Q S_0)^*(y(t) - \hat{y}(t)) + A_Q R_0(u(t+1) - \hat{u}(t+1)) \\
&\quad + B_Q[B_M^*(y(t) - \hat{y}(t)) - A_M(u(t+1) - \hat{u}(t+1))].
\end{aligned}
\quad (54)
$$

Taking into consideration eqs. (10), (48)

$$
\begin{aligned}
B_Q[B_M^*(y(t) - \hat{y}(t)) - A_M(u(t+1) - \hat{u}(t+1))] &= \\
= B_Q\left[B_M^*\varepsilon(t) - A_M\frac{B_M^*}{A_M}\varepsilon(t)\right] &= 0
\end{aligned}
\quad (55)
$$

and dividing equations (50), (54) one obtains

$$
\begin{aligned}
\varepsilon(t+1) &= -((-A_Q + \hat{A}_Q)S_0)^*\hat{y}(t) + (-A_Q + \hat{A}_Q)R_0\hat{u}(t+1) \\
&\quad + (-B_Q + \hat{B}_Q)[B_M^*\hat{y}(t) - A_M\hat{u}(t+1)] \\
&\quad - (A_Q S_0)^*\varepsilon(t) + A_Q R_0\frac{B_M^*}{A_M}\varepsilon(t).
\end{aligned}
\quad (56)
$$

Passing the terms in $\varepsilon(t)$ on the left hand side

$$
\begin{aligned}
\left[1 + q^{-1}\left(\frac{A_M(A_Q S_0)^* - A_Q R_0 B_M^*}{A_M}\right)\right]\varepsilon(t+1) &= \frac{A_Q P_0}{A_M}\varepsilon(t+1) \\
= -(-A_Q^* + \hat{A}_Q^*)[S_0\hat{y}(t) + R_0\hat{u}(t)] & \\
+ (-B_Q + \hat{B}_Q)[B_M\hat{y}(t+1) - A_M\hat{u}(t+1)] &
\end{aligned}
\quad (57)
$$

Using eqs. (53) and (21)one gets eq. (17) and this ends the proof.

REFERENCES

[1] M. Alma, J.J. Martinez, I.D. Landau, and G. Buche. Design and tuning of reduced order h-infinity feedforward compensators for active vibration control. Internal report, GIPSA-Lab Grenoble France, 2010.

[2] B.D.O. Anderson. From Youla-Kucera to identification, adaptive and nonlinear control. *Automatica*, 34:1485–1506, 1998.

[3] S.J. Elliott and P.A. Nelson. Active noise control. *Noise / News International*, pages 75–98, June 1994.

[4] S.J. Elliott and T.J. Sutton. Performance of feedforward and feedback systems for active control. *IEEE Transactions on Speech and Audio Processing*, 4(3):214–223, May 1996.

[5] G.C. Goodwin and K.S. Sin. *Adaptive Filtering Prediction and Control*. Prentice Hall, N. J., 1984.

[6] J Hu and J.F Linn. Feedforward active noise controller design in ducts without independent noise source measurements. *IEEE transactions on control system technology*, 8(3):443–455, 2000.

[7] C.A Jacobson, C.R Johnson, D.C Mc Cormick, and W.A Sethares. Stability of active noise control algorithms. *IEEE Signal Processing letters*, 8(3):74–76, 2001.

[8] M.S. Kuo and D.R. Morgan. *Active noise control systems-Algorithms and DSP implementation*. Wiley, New York,, 1996.

[9] I.D. Landau, T.B. Airimiţoaie, and M. Alma. A youla-kucera parametrized adaptive feedforward compensator for active vibration control. In *Proceedings of the 18th IFAC World Congress, Milano, Italy*, 2011.

[10] I.D. Landau, M. Alma, and T.B. Airimiţoaie. Adaptive feedforward compensation algorithms for active vibration control with mechanical coupling. *Automatica*, 2011. DOI: 10.1016/j.automatica.2011.08.015.

[11] I.D. Landau and A. Karimi. Recursive algorithms for identification in closed loop. a unified approach and evaluation. *Automatica*, 33(8):1499–1523, 1997.

[12] I.D. Landau, A. Karimi, and A. Constantinescu. Direct controller order reduction by identification in closed loop. *Automatica*, 37:1689–1702, 2001.

[13] I.D. Landau, R. Lozano, and M. M'Saad. *Adaptive control*. Springer, London, 1997.

[14] L Ljung and T Söderström. *Theory and practice of recursive identification*. The M.I.T Press, Cambridge Massachusetts , London, England, 1983.

[15] A.K. Wang and W. Ren. Convergence analysis of the filtered-u algorithm for active noise control. *Signal Processing*, 73:255–266, 1999.

[16] J Zeng and R.A de Callafon. Recursive filter estimation for feedforward noise cancellation with acoustic coupling. *Journal of sound and vibration*, 291:1061–1079, 2006.